



# Kinetics of the hydration reactions in the cement paste with mechanochemically modified cement <sup>29</sup>Si magic-angle-spinning NMR study

Karin Johansson<sup>a</sup>, Cecilia Larsson<sup>a</sup>, Oleg N. Antzutkin<sup>a,\*</sup>, Willis Forsling<sup>a</sup>,  
Hanumantha Rao Kota<sup>b</sup>, Vladimir Ronin<sup>c</sup>

<sup>a</sup>*Division of Inorganic Chemistry, Luleå University of Technology, S-971 87 Luleå, Sweden*

<sup>b</sup>*Division of Mineral Processing, Luleå University of Technology, S-971 87 Luleå, Sweden*

<sup>c</sup>*Division of Structural Engineering, Luleå University of Technology, S-971 87 Luleå, Sweden*

Received 29 September 1998; accepted 7 June 1999

## Abstract

A comparative <sup>29</sup>Si solid state NMR study of kinetics of the hydration reactions in cement pastes based on rapid-hardening ordinary Portland cement (SH) and on the mechanochemically modified cement (MSH) is presented. The mechanical activation of a cement/silica fume blend in a vibrating mill accelerates the hydration reactions by 15–20%, especially during the initial period of hardening. Variations in relative intensities of <sup>29</sup>Si resonances assigned to the hydration products in SH/MSH blends suggest different structures of hydrated SH nets. This can be correlated with a pronounced increase of the MSH-cement binding capacity reported earlier. © 1999 Elsevier Science Ltd. All rights reserved.

**Keywords:** Hydration; Kinetics; <sup>29</sup>Si-MAS-NMR spectroscopy; Cement paste; Silica fume

## 1. Introduction

Modern concrete technology requires further enhancement of the Portland cement-based binders due to increased building demands. New types of cements can be produced with milling-vibrating equipment by high intensive mechanochemical treatment of the Portland cement with silica fume or other silicon-oxide-containing additives [1]. This new product, called “energetically modified cement” (EMC), has a higher surface reactivity and better mechanical properties than ordinary Portland cement (OPC) [2–5]. Due to the mechanochemical activation a significant increase of strength development and ultimate strengths of EMC-mortars and concretes (up to 180 MPa) occurs. A reduction of porosity and an increase of durability also have been observed [4,5].

Jonasson et al. reported the increase of chemical reactivity of the EMC binder compared with the use of nonmodified cement as measured by the X-ray diffraction [3,4]. The intensity of Ca(OH)<sub>2</sub> and C<sub>3</sub>S peaks were much lower in the EMC binder compared with OPC after 2 years of hardening; this indicated the increased rate of both pozzolanic and hydration reactions [3,4].

Searching for the mechanism of the mechanochemical activation, Rao Kota et al. performed a comparative study of EMC and OPC blends using diffuse reflectance Fourier transformed infrared (FT-IR) spectroscopy [5]. The spectral features of the blends have been found to be exactly the same before and after vibration milling. However, after the modification process the intensity of the silica fume bands rose, which was obviously due to the increase in the surface area of silica fume by deagglomeration and its dispersion [5]. This conclusion has been also supported by scanning electron microscope (SEM) studies: Submicro silica fume particles were homogeneously distributed/attached over the EMC grains [4].

During the last decade the solid state nuclear magnetic resonance (NMR) spectroscopy has emerged as a powerful analytical technique for structural investigations in chemistry of cements and concretes [6,7]. A large number of solid state NMR studies were carried out to show how the degree of hydration is correlated with the connection of the silicate species [8,9] and with the compressive strength of cement pastes [10]. Various interesting aspects of the cement hydration reactions such as the addition of siliceous material and carbonation of various types of cement mixtures have been examined and useful results obtained [11].

Natural abundance <sup>29</sup>Si solid state NMR has found a wide application in cement chemistry. For the silicates the chemi-

\* Corresponding author. Tel.: +46-920-72524; fax: +46-920-91199.  
E-mail address: olan@km.luth.se (O.N. Antzutkin)

cal shift of the resonance of the  $^{29}\text{Si}$  nucleus gives a relatively clear indication of the number of bridging oxygens in a particular  $\text{SiO}_4$  unit. Increasing numbers of bridging oxygens per tetrahedron (i.e., increased polymerization) results in shifts to higher fields (increased shielding of  $^{29}\text{Si}$  nuclei by surrounding electrons). Different  $Q^n$  sites ( $Q$  represents the silicate tetrahedron and  $n$  refers to the number of other tetrahedra to which it is linked by the sharing of oxygens) have distinct regions of  $^{29}\text{Si}$  chemical shifts in solid silicates [centered at:  $Q^0$ ,  $-70$  ppm;  $Q^1$ ,  $-80$  ppm;  $Q^2$ ,  $-88$  ppm;  $Q^3$ ,  $-98$  ppm; and  $Q^4$ ,  $-110$  ppm—all shifts are given from tetramethylsilane (TMS)] [12]. Integrated peak intensity can be used to estimate relative amounts of different  $Q$  sites in solid silicates and, therefore, to quantify the degree of polymerization and connectivities in the micronet of hydrated cements. It has been shown that the  $Q^1/Q^2$  ratio in the hydrated cement materials decreases with time but  $Q^3$  and  $Q^4$  units do not appear. This has been found to be true for  $\text{C}_3\text{S}$  ( $3\text{CaO} \cdot \text{SiO}_2$ ) pastes hydrated up to 26 years [13]. A correlation between the length of the chains in CSH (hydrated OPC) and the stoichiometric ratio  $\text{Ca}/\text{Si}$  has been also recently established [14]. Al-Dulaijan et al. found a correlation between the compressive strength of cement pastes and the spatial distribution of the hydration products (and therefore the  $Q^1/Q^2$  ratio) [15].

In this work we report a comparative  $^{29}\text{Si}$  solid state NMR study of the kinetics of hydration reactions in rapid-hardening ordinary Portland cement (SH, from “snabbhårdande,” Swedish) and mechanochemically activated cement (MSH) pastes. By these studies we confirm previous conclusions that the modification process accelerates the hydration reaction.  $^{29}\text{Si}$  spectra also reveal structural differences between hydrated SH and MSH pastes.

## 2. Methods

### 2.1. Materials

The pure SH, produced by Cementa AB (Slite, Sweden), calcium silicates  $2 \text{CaO} \cdot \text{SiO}_2$  ( $\text{C}_2\text{S}$ ), and  $3 \text{CaO} \cdot \text{SiO}_2$  ( $\text{C}_3\text{S}$ ) were used in this work. Condensed silica fume (SF) produced by Elkem A/S (Norway) as a pozzolanic additive was used in the experiments. The chemical composition of these materials is shown in Table 1.

### 2.2. Mechanical activation

The mechanical activation of the blend (95 wt% SH cement and 5 wt% silica fume) was carried out in a Humboldt Palla 20U vibrating mill (Humboldt, Germany). A blend of 2 kg of material was subjected to milling for 30 min with porcelain cylindrical grinding media.

### 2.3. Sample preparation

The blends before and after mechanical activation were used for the preparation of cement paste specimens for the follow-up hydration studies by magic-angle-spinning (MAS) NMR. Cylindrical paste specimens with the diameter of 25

Table 1

Chemical composition of the materials

Oxide	SH cement (wt%)	Silica fume (wt%)
$\text{SiO}_2$	19.80	96.00
$\text{Al}_2\text{O}_3$	4.23	0.30
$\text{Fe}_2\text{O}_3$	2.21	0.20
$\text{CaO}$	63.00	0.95
$\text{MgO}$	3.43	0.30
$\text{SO}_3$	3.23	0.10
$\text{K}_2\text{O}$	1.28	0.30
$\text{NaO}$ , $\text{MnO}$ , $\text{TiO}_2$	0.27	0.20
BET surface area ( $\text{m}^2\text{g}^{-1}$ )	1.830	19.74

mm and the length of 55 mm were produced with water-binder ratio of 0.25 and 0.40 for the nonactivated and activated blends. The nonactivated blend was thoroughly homogenized in a rotating drum prior to the preparation of the paste specimen. For each blend, five specimens were prepared in a polyethylene container and were heated at  $110^\circ\text{C}$  after curing times of 1, 3, 7, 14, and 28 days, respectively, to stop the hydration reaction. The specimens were then crushed and powdered to less than about  $20\text{-}\mu\text{m}$  size. The powdered samples were washed with ethanol, once again heated to remove any trace of water, and stored in a deep-freeze at  $-25^\circ\text{C}$  until they were used for MAS NMR spectral studies.

### 2.4. NMR measurements

Solid state  $^{29}\text{Si}$  MAS NMR spectra were recorded on a Chemagnetics Infinity CMX-360 ( $B_0 = 8.46 \text{ T}$ ) spectrometer (Varian, USA) using a single pulse experiment without proton decoupling. The  $^{29}\text{Si}$  operating frequency was 71.5085 MHz. The silicon  $70^\circ$  pulse duration was 4.5  $\mu\text{s}$ . For different samples 2048 or 4096 transients with a relaxation delay of 3 s were accumulated. These delays were 5 to 10 times longer than  $T_1$  relaxation times of  $^{29}\text{Si}$  sites in cement/silica fume blends under study.  $T_1$  relaxation times of different  $^{29}\text{Si}$  sites were measured using the standard inversion recovery experiment ( $180^\circ\text{-}\tau\text{-}90^\circ\text{-acq}$ ) [16]. In these experiments  $90^\circ$  and  $180^\circ$  pulse durations were 6.4 and 12.8  $\mu\text{s}$ , respectively. Powder samples (approximately 750 mg for unhydrated blends and 500–550 mg for hydrated blends) were packed into zirconium dioxide standard double bearing 7.5-mm rotors. The spinning frequency for all samples was 6000 Hz and was stabilized to  $\pm 3 \text{ Hz}$  using an internal stabilization device. All  $^{29}\text{Si}$  chemical shift data were externally referenced to the TMS resonance.

All solid state  $^{29}\text{Si}$  MAS NMR spectra were recorded at room temperature (approximately 300 K).

## 3. Results and discussion

To estimate the composition of blends used in our studies,  $^{29}\text{Si}$  MAS NMR experiments on crystalline calcium silicates  $\text{C}_2\text{S}$  and  $\text{C}_3\text{S}$  were carried out (Fig. 1, patterns a and b). It is known that there are four different  $\text{C}_2\text{S}$  conformers and that each of them has just one silicone site in an isolated

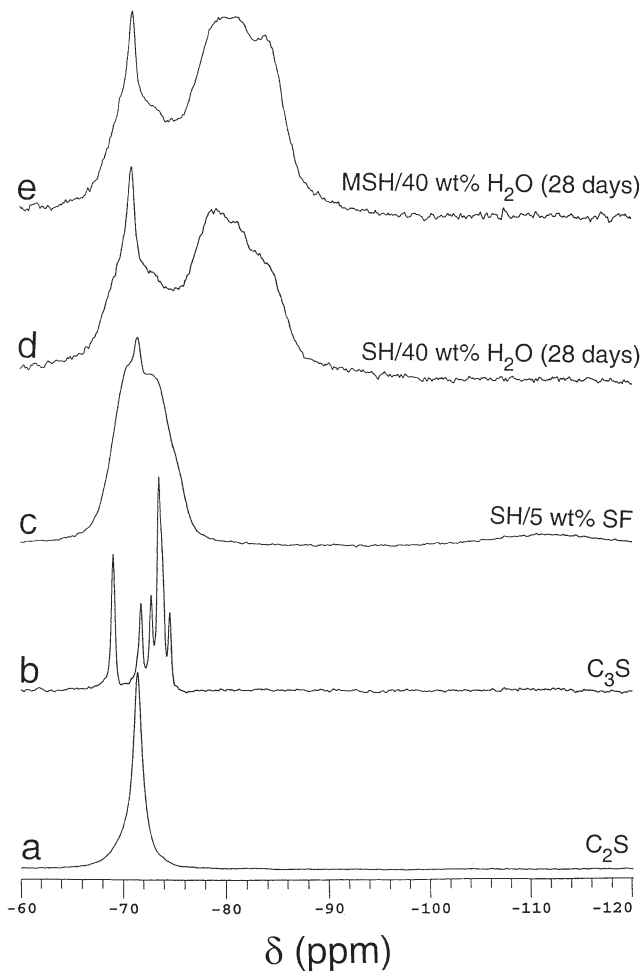


Fig. 1. The 71.5805 MHz  $^{29}\text{Si}$  single-pulse MAS NMR spectra of the following compounds. Pattern a,  $2\text{CaO} \cdot \text{SiO}_2$ ; pattern b,  $3\text{CaO} \cdot \text{SiO}_2$ ; pattern c, homogenized mixture of 95 wt% SH and 5 wt% of the SF; pattern d, as in pattern c, but after 28 days of the hydration with 40 wt% of water in the cement paste; pattern e, as in pattern d, but the blend was mechanically activated during 30 min before the hydration. The MAS frequency was 6 kHz. The number of transients was 2048 (patterns a–c) and 4096 (patterns d, e).

$\text{SiO}_4^{4-}$  tetraeder ( $\text{Q}^0$  site), giving rise to a single resonance at  $-70.7$  ppm ( $\alpha\text{-C}_2\text{S}$ ),  $-70.8$  ppm ( $\alpha'_L\text{-C}_2\text{S}$ ),  $-71.4$  ppm ( $\beta\text{-C}_2\text{S}$ , larnite), or  $-73.5$  ppm ( $\gamma\text{-C}_2\text{S}$ , bredigite) [17,18]. In turn,  $\text{C}_3\text{S}$ -T triclinic phase is represented by nine different Si sites in the asymmetric unit (also  $\text{Q}^0$  sites) [19] giving rise to seven resolved resonances at  $-69.2$ ,  $-71.9$ ,  $-72.9$ ,  $-73.6$ ,  $-73.8$ ,  $-74.0$ , and  $-74.7$  ppm with relative intensities 2:1:1:2:1:1:1 [17,20,21]. Fig. 1 (pattern a) shows a single resonance at  $-70.7$  ppm, which can be assigned here to the known  $\beta\text{-C}_2\text{S}$  conformer. However, the resonance is quite broad, indicating a relatively low crystallinity of the sample. NMR spectrum of  $\text{C}_3\text{S}$  (Fig. 1, pattern b) consists of five resolved peaks at  $-69.1$ ,  $-71.8$ ,  $-72.8$ ,  $-73.6$ , and  $-74.6$  ppm with relative integrated intensities of 2:1:1:4:1. Again, the positions of all peaks are the same as reported earlier [17,20,21]. The most intensive peak in Fig. 1 (pattern b)

corresponds to the three overlapping resonances that are not resolved in our sample.

Fig. 1 (pattern c) shows the  $^{29}\text{Si}$  spectrum of the binder of 95 wt% rapid-hardening ordinary Portland cement with 5 wt% of the silica fume. Since this is a mechanical mixture of two substances, two separate resonances are clearly detected: a broad resonance around  $-111$  ppm ( $\text{SiO}_2$ ,  $\text{Q}^4$  sites) [22] and a broad, partly resolved resonance between  $-69$  and  $-76$  ppm ( $\text{Q}^0$  sites). The latter consists mainly of broad overlapping  $\text{C}_3\text{S}$ , alite ( $\sim 65$  wt%), and  $\text{C}_2\text{S}$ , belite ( $\sim 11.7$  wt%) resonances (see Tables 1 and 2). After the mechanical activation in the vibrating mill of the cement/silica fume blend, its  $^{29}\text{Si}$  NMR spectrum did not change. This suggests no chemical modification of the blend on the molecular level. However, this result does not exclude a possible modification of silicone sites on the surface of cement particles: the  $^{29}\text{Si}$  NMR signal of the surface monolayer is screened by the signal that is three orders of magnitude larger from silicone sites in the bulk.

Fig. 1 (patterns d and e) shows  $^{29}\text{Si}$  spectra of the hydrated blends after 28 days from the beginning of the hydration reaction. Both samples were prepared from the cement pastes 95 wt% SH and 5 wt% SF with water/binder ratio of 0.4. The modified SH cement/silica fume blend (MSH) (Fig. 1, pattern e) was prepared by mechanical activation for 30 minutes in the vibrating mill before hydration. There are two distinct features in the spectra of the hydrated blends: (1) a new, broad resonance appears between  $-75$  and  $-88$  ppm, which corresponds to  $\text{Q}^1$  and  $\text{Q}^2$  Si sites in the  $-\text{O}-\text{Si}-\text{O}-$  net of the hydrated amorphous products. Since the chemical environment around silicone sites varies, this signal is a poorly resolved broad singlet; and (2) the shape of the “initial” cement signal is changed dramatically with the  $\text{C}_3\text{S}$  component of the signal, considerably suppressed compared to the  $\text{C}_2\text{S}$  peak. The latter reflects the well-known fact that  $\text{C}_3\text{S}$  is a fast-reacting component in cement blends (the half-time of the reaction is a few hours), while  $\text{C}_2\text{S}$  reacts with water rather slowly (months) [23]. Comparing  $^{29}\text{Si}$  NMR spectra of the hydrated binders with (Fig. 1, pattern e) and without (Fig. 1, pattern d) the mechanical activation, one can conclude that: (1) more hydrated products are built in the first (mechanically activated) system; (2) NMR signal in the interval  $(-83, -88$  ppm), which can be assigned to  $\text{Q}^2$  sites [12], is approximately twice as large in the MSH/SF sample. Two important conclusions can be drawn from this analysis: the hydration proceeds faster in the mechanically activated MSH/SH system and the relative ratio  $\text{Q}^2/\text{Q}^1$  is also larger for the MSH/SF

Table 2  
The estimated chemical composition of SH

Phase	Composition (wt%)
$\text{C}_3\text{S}$ ( $3\text{CaO} \cdot \text{SiO}_2$ )	$\approx 65$
$\text{C}_2\text{S}$ ( $2\text{CaO} \cdot \text{SiO}_2$ )	$\approx 11.7$
$\text{C}_3\text{A}$ ( $3\text{CaO} \cdot \text{Al}_2\text{O}_3$ )	$\approx 11.5$
$\text{C}_4\text{AF}$ ( $4\text{CaO} \cdot \text{Al}_2\text{O}_3 \cdot \text{Fe}_2\text{O}_3$ )	$\approx 7.3$

paste [estimated from peak intensities at  $-78.9$  ppm ( $Q^1$ ) and  $-84.4$  ppm ( $Q^2$ ):  $Q^2/Q^1$  (SH/SF) = 0.65,  $Q^2/Q^1$  (MSH/SF) = 0.9]. It is known that the high compressive strength of cement pastes and concretes can be correlated with a high value of the  $Q^2/Q^1$  ratio [15]. In our case this confirms the outstanding properties of the MSH/SF cement pastes reported earlier [2–5]. However, we have to stress that this conclusion is more qualitative, rather than quantitative: It is difficult to calculate the exact ratio  $Q^2/Q^1$  because of a severe broadening/overlap of the resonances in the hydrated blends.

The comparative hydration kinetics of the nonactivated SH/SF and MSH/SF blends are shown in Figs. 2 and 3. In the first and second cases water/binder ratios were 0.25 and 0.4, respectively. All spectra are plotted in the corresponding scales, which were calculated from the normalization on the weight of each sample and the number of transients. These scalings were also proven to be correct by comparing total integrated signals among different spectra. We disregarded the possibility of the saturation effects in our measurements since  $T_1$  relaxation times measured in the inversion recovery experiment were between 300 and 400 ms for all  $^{29}\text{Si}$  sites in the unhydrated and hydrated samples (with one exception for the silica fume resonances that have  $T_1 \sim 720$  ms). These relaxation times were 5 to 10 times shorter than the repetition time of 3 s employed. We also

used  $70^\circ$  instead of  $90^\circ$  pulse to further avoid any small saturation effects. The fast spin-lattice relaxation in the systems under study can be explained by the presence of paramagnetic metal ions, Fe(III) and Mn(II) (see Table 1) [16]. Spectra of unhydrated (Fig. 2, patterns a and a', and Fig. 3, patterns a and a') and hydrated (Figs. 2, patterns b to f, b' to f', and Fig. 3, patterns b to f, b' to f') blends have different signal-to-noise ratios because of larger weights of samples of unhydrated blends (750 mg compared with 500–550 mg for the hydrated samples).

Referring to the arguments mentioned above, all spectra in Figs. 2 and 3 can be directly compared and quantitatively analyzed in terms of the time dependence of signals integrated in the chosen intervals,  $-65$ ,  $-75$  ppm for reagents and  $-75$ ,  $-95$  ppm for hydrated products. The effect of the mechanical activation is expressed by the considerable rise of signals of the hydrated products. Moreover, this effect is more pronounced for pastes with water/binder ratio of 0.4 (Fig. 3), which can be connected with higher amount of water available for hydration.

To perform the quantitative analysis of the hydration kinetics all spectra were deconvoluted (using the built-in "Spin-sight" software of the spectrometer) with the simulation peaks at  $-69.2$ ,  $-71.4$ ,  $-72.0$ ,  $-73.5$  ppm for unhydrated  $^{29}\text{Si}$  sites;  $-78.9$ ,  $-81.5$ ,  $-84.4$ ,  $-91$  ppm for the hydrated

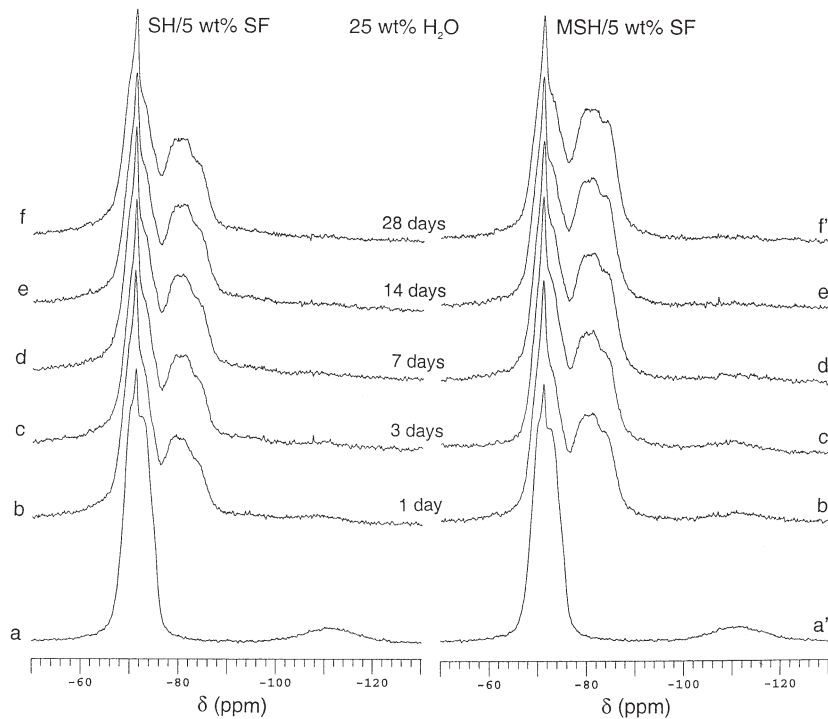


Fig. 2. The comparative hydration reaction kinetics of blends constituting of 95 wt% SH and 5 wt% of the SF with water-binder ratio of 0.25. Pattern a (non-activated) and pattern a' (MSH/SF), before the hydration. The hydration reactions were stopped after 1 (patterns b, b'); 3 (patterns c, c'); 7 (patterns d, d'); 14 (patterns e, e'), and 28 days (patterns f, f') from the beginning of the hydration. The  $^{29}\text{Si}$  MAS NMR spectra were obtained at the spinning frequency of 6 kHz with the number of transients equal to 2048 (patterns a, a') and 4096 (patterns b–f, b'–f'). Scaling factors for each spectrum were obtained from the normalization on weights and the number of transients (see text for details). Weights of the samples were approximately 750 mg (patterns a, a') and 500–550 mg (patterns b–f, b'–f').

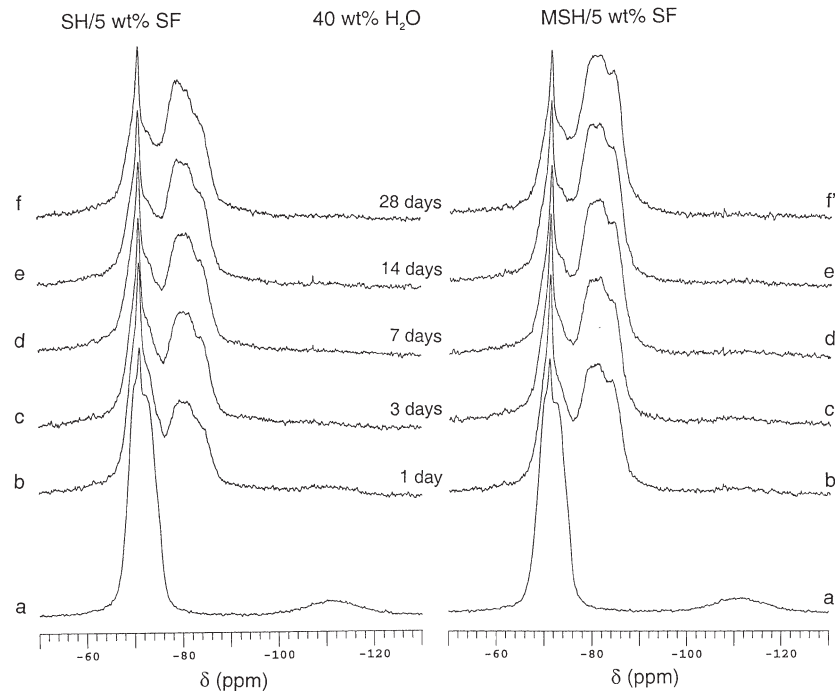


Fig. 3. The same as in Fig. 2 but with water-binder ratio of 0.4.

$Q^1$  and  $Q^2$  sites; and  $-111$  ppm for the  $Q^4$  sites of silica fume. Sums of integrals of the simulated peaks in the each group of resonances were used in the kinetics plots. Deviations of the sum of integrals of all simulated peaks from the total integral of the experimental spectra were always less than 3 %. We also found that this deconvolution procedure is more accurate compared to the integrating of experimental spectra in the chosen intervals,  $-65$ ,  $-75$  ppm, corresponding roughly to unhydrated silica sites, and  $-75$ ,  $-95$  ppm, to hydrated products. The latter procedure was found to be unfavorable because of a larger dependence of integrals to the used phase and baseline corrections of the spectra.

The hydration kinetics are plotted in Figs. 4 and 5. It can be noted that the main difference in the kinetics takes place at the very beginning of the hydration reaction (up to 3 days) and then both curves (nonactivated SH and mechanically activated MSH blends) are almost parallel. It can be concluded that the mechanical activation accelerates considerably (by approximately 12% at water/binder ratio of 0.25 and by approximately 22% at 40 wt% of  $H_2O$ ), the hydration reaction of the fast (i.e.,  $C_3S$ ) component of the cement/silica fume binder. The most reasonable explanation of this is the homogenization/redistribution on the microscopical level of small silica fume particles in the vicinity of  $C_3S$  crystals, which are approximately two orders of magnitude larger in size [4,5]. This fine redistribution can be guaranteed only by an extensive mechanical activation of cement blends in the vibrating mill. When the microscopical homogeneity is reached, the proper mixture of  $C_3S$  and SF guarantees the excessive acceleration of the pozzolanic reaction between  $Ca(OH)_2$  (which builds up at the particle surfaces during the initial hydration

reaction of  $C_3S$ ) and  $SiO_2$ . As a result,  $H_2O$  molecules are not hampered by  $Ca(OH)_2$  crystals and can therefore diffuse further to the  $C_3S$  particles. More extensive nets of the hydrated products are formed and the compressive strength of cement pastes/concretes rises considerably. The redistribution and disintegration of silica fume grains also lead to building up of effective nuclei sites, considerably promoting the formation of CSH nets especially at early stages of hardening. This conclusion is supported by our present results that show the increased intensity of signals from  $Q^2$  silica sites in the hydrated, mechanically activated blends. It is known that the CSH formed by hydration of calcium silicates is generally dominated by  $Q^1$  sites or has  $Q^1$  and  $Q^2$  sites in nearly equal abundance. When a source of silica such as silica gel or silica fume is present,  $Q^2$  sites are more abundant than  $Q^1$  sites [24].

We do not exclude the possibility that the intensive mechanical activation has a direct impact on the surface layers of  $C_3S$  minerals, which become more thermodynamically unstable due to the high intensive solid-solid interaction with silica fume particles and grinding media during the activation process. These hypotheses are currently under experimental testing using pure model systems of mechanically activated blends of  $CaO$ ,  $C_2S$ , or  $C_3S$  with the silica fume.

#### 4. Conclusions

Using  $^{29}Si$  solid state NMR spectroscopy it was shown that the mechanical activation of cement/silica fume blends in a vibrating mill accelerates the hydration reaction by 15–20%, especially during the initial period of hardening, and

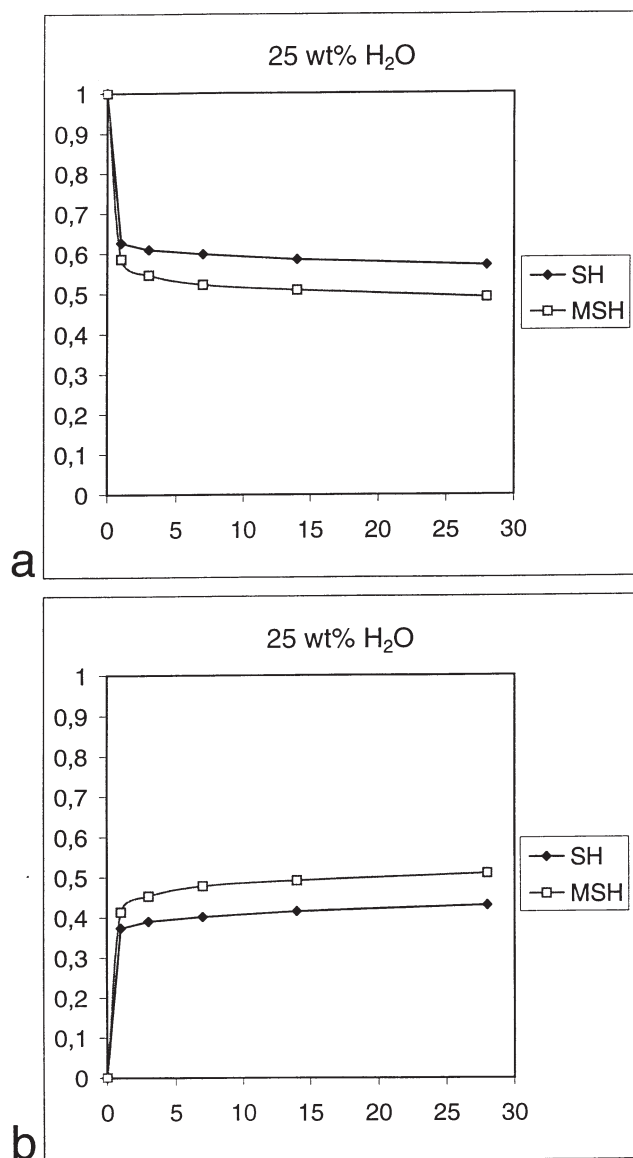


Fig. 4. Plots of the hydration reaction kinetics for nonactivated (diamonds) and mechanically activated (squares) blends described in Fig. 2. The water-binder ratio is equal to 0.25. X-axis is given in days, while y-axis is the normalized on the total integral  $^{29}\text{Si}$  NMR signal from (pattern a) unhydrated and (pattern b) hydrated sites. Sums of integrals of deconvoluted peaks at  $-69.2$ ,  $-71.4$ ,  $-72.0$ ,  $-73.5$  ppm for unhydrated and  $-78.9$ ,  $-81.5$ ,  $-84.4$ ,  $-91$  ppm for hydrated  $^{29}\text{Si}$  sites were used in each case.

was more pronounced at high water/binder ratios of 0.4. The ratio,  $Q^2/Q^1$ , of silicone sites in the hydrated products also rises after the mechanical activation of blends, which can be correlated with the high compressive strengths of the mechanochemically activated cement pastes. The hypothesis of the fine homogenization/redistribution of small silica fume particles with the formation of thin  $\text{SiO}_2$  layers around  $\text{C}_3\text{S}$  crystals that accelerates the pozzolanic reaction and promotes growing of more extensive nets of the hydrated products is suggested.

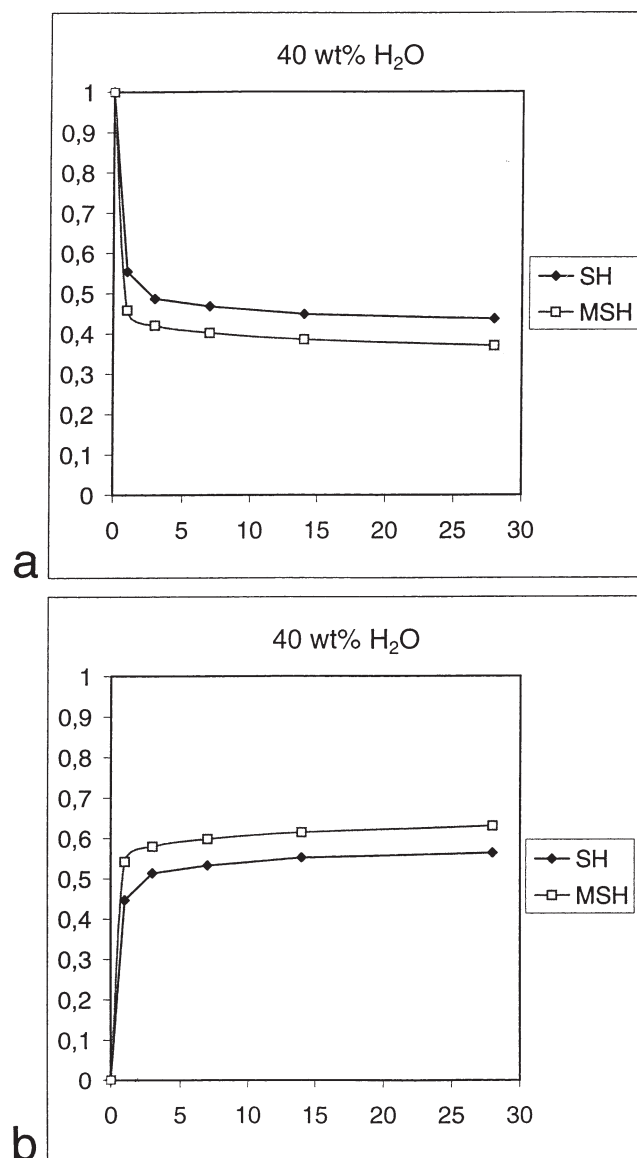


Fig. 5. The same as in Fig. 4 but with water-binder ratio of 0.4.

## Acknowledgment

We acknowledge Swedish Council for planning and co-ordination of Research (FRN) for a grant for the CMX-360 NMR spectrometer.

## References

- [1] V. Ronin, M. Häggström, Method for producing cement, International patent application, PCT/SE94/00383.
- [2] V. Ronin, J.-E. Jonasson, High strength and high performance concrete with use of EMC hardening at cold climate conditions, Proceedings of International Conference on Concrete under Severe Conditions, Sapporo, Japan, August 1995.
- [3] J.-E. Jonasson, V. Ronin, H. Hedlund, High strength concretes with energetically modified cement and modeling of shrinkage caused by self-desiccation, Proceedings of the 4th International Symposium on the Uti-

- lization of High Strength/High Performance Concrete, Paris, France, August 1996, Presses Pont et Chaussees, Paris, 1996, pp. 245–254.
- [4] V. Ronin, J.-E. Jonasson, H. Hedlund, Advanced modification technologies of the Portland cement based binders for different high performance applications, Proceedings of the 10th International Congress of the Chemistry of Cements, Gothenburg, Sweden, June 1997.
  - [5] H. Rao Kota, V. Ronin, E. Forssberg, High performance energetically modified Portland blast-furnace cements, Proceedings of the 10th International Congress of the Chemistry of Cements, Gothenburg, Sweden, June 1997.
  - [6] P. Colombet, A.-R. Grimmer (Eds.), Application of NMR Spectroscopy to Cement Science, Gordon and Breach, London, 1994.
  - [7] P. Colombet, A.-R. Grimmer (Eds.), Nuclear Magnetic Resonance Spectroscopy of Cement Based Materials, Springer Verlag, Berlin, Heidelberg, 1998.
  - [8] N.J. Clayden, C.M. Dobson, C.J. Hayes, S.A. Roger, Hydration of tricalcium silicate followed by solid-state  $^{29}\text{Si}$  NMR spectroscopy, J Chem Soc Chem Commun (1984) 1396–1397.
  - [9] Y. Tong, H. Du, L. Fei, Hydration process of beta-dicalcium silicate followed by MAS and CP/MAS NMR, Cem Concr Res 21 (1991) 355–358.
  - [10] G. Parry-Jones, A.-H.J. Al-Tayyib, S.U. Al-Dulaijan, A.I. Al-Manna,  $^{29}\text{Si}$  MAS NMR hydration and compressive strength study in cement paste, Cem Concr Res 19 (1989) 228–234.
  - [11] S.A. Rodger, The use of solid state NMR in the study of cement hydration, RILEM Proc 16 (1992) 65–76.
  - [12] E. Lippmaa, M. Mägi, A. Samoson, G. Engelhardt, A.-R. Grimmer, Structural studies of silicates by solid-state high-resolution  $^{29}\text{Si}$  NMR, J Am Chem Soc 102 (1980) 4889–4893.
  - [13] S.A. Rodger, G.W. Groves, N.J. Clayden, C.M. Dobson, A study of tricalcium silicate hydration from very early to very late stages, Mat Res Soc Symp Proc 85 (1987) 13–20.
  - [14] B. Bresson, S. Masse, H. Zanni, Proton observation in calcium silicate hydrates by CRAMPS technique, XIII European Experimental NMR Conference (EENC), Paris, France, May 19–24, 1996, p. 432.
  - [15] S.U. Al-Dulaijan, G. Parry-Jones, A.-H.J. Al-Tayyib, A.I. Al-Manna,  $^{29}\text{Si}$  MAS NMR study of hydrated cement paste and mortar, J Am Ceram Soc 73 (3) (1990) 736–739.
  - [16] D.D. Traficante, Relaxation: An introduction, in: Encyclopedia of Nuclear Magnetic Resonance, vol. 6, D. M. Grant, R. K. Harris (Eds.), Wiley, New York, 1996, pp. 3988–4003.
  - [17] A.-R. Grimmer, Structural investigation of calcium silicates from  $^{29}\text{Si}$  chemical shift measurements, in: P. Colombet, A.-R. Grimmer (Eds.), Application of NMR Spectroscopy to Cement Science, Gordon and Breach, London, 1994, pp. 113–151.
  - [18] A.-R. Grimmer, F. von Lampe, M. Mägi, E. Lippmaa, High-resolution solid-state  $^{29}\text{Si}$  NMR of polymorphs of  $\text{Ca}_2\text{SiO}_4$ , Cem Concr Res 15 (1985) 467.
  - [19] N.I. Golovastikov, R.G. Matveeva, V. Belov, Crystal structure of the tricalcium silicate  $3\text{CaO} \cdot \text{SiO}_2$  ( $\text{C}_3\text{S}$ ), Sov Phys Crystallogr 20 (4) (1976) 441–445.
  - [20] R. Rassem, Apport de la RMN à l'étude du mécanisme d'hydratation du silicate tricalcique, Ph.D. Thesis, Paris Université Pierre et Marie Curie, 1990.
  - [21] E. Lippmaa, M. Mägi, M. Tarmak, W. Wieker, A.-R. Grimmer, Solid-state high-resolution  $^{29}\text{Si}$  NMR study of the hydration of  $\text{C}_3\text{S}$ , Cem Concr Res 12 (1982) 597–602.
  - [22] M. Lajnef, H. Taïbi, A.P. Legrand, H. Hommel, Characterization of silica fume by  $^{29}\text{Si}$  NMR, in Application of NMR Spectroscopy to Cement Science, P. Colombet, A.-R. Grimmer (Eds.), Gordon and Breach, London, 1994, pp. 181–188.
  - [23] F.M. Lea, The Chemistry of Cement and Concrete, 3d ed., Bell and Bain Ltd., Glasgow, 1970.
  - [24] J. Hjorth, J. Skipsted, J. Jakobsen,  $^{29}\text{Si}$  MAS NMR studies of Portland cement components and effects of microsilica on the hydration reaction, Cem Concr Res 18 (1988) 789–798.